AIAA 82-4187

A Rapid Approximation Procedure for Nonlinear Solutions: Application to Aerodynamic Flows

Stephen S. Stahara* and James P. Elliott†
Nielsen Engineering and Research, Inc., Mountain View, Calif.
and
John R. Spreiter‡
Stanford University, Stanford, Calif.

A method for determining accurate approximations to strongly nonlinear solutions that are either continuous or discontinuous is developed and evaluated. The concept of coordinate straining suggested by Nixon is used to account for displacement of discontinuities and maxima of high-gradient regions due to parameter variation. Comparisons with "exact" nonlinear solutions are presented for a variety of aerodynamic flows which demonstrate the remarkable accuracy of the procedure and illustrate its range of validity in typical applications. Attention is focused on strongly supercritical transonic flows that exhibit large surface shock movement over the parametric range studied. Comparisons employing different classes of straining functions indicate the superiority of linear piecewise continuous functions.

Introduction

WITH the growing capability of advanced computational procedures to simulate a variety of complex phenomena, it is clear that a need exists for complimentary methods capable of alleviating, at least in part, the usage limitations imposed on these methods by their computational expense. The need becomes particularly compelling when large numbers of related solutions are required as in parametric or design studies. Techniques which enhance the efficiency of the solution algorithms represent only a partial answer. What is most desirable is a means for minimizing the number of separate computationally expensive solutions required in a particular application by extending the usefulness of each individual solution over some parametric range.

The classical approach of accomplishing this, involving the establishing and solving of a series of linear perturbation problems, appears as an obvious choice. Recent studies,[1] however, have shown that, for applications to sensitive flows such as typically occur in transonic situations, the fundamental linear assumption of that technique is sufficiently restrictive that the useful range of parameter variations is so small as to be of little practical use. An interesting alternative recently has been examined[1-5] successfully, in which an approximation technique is used that employs two or more base solutions determined by the full computational method to predict entire families of related nonlinear solutions. In the initial demonstration of the method,[2] Nixon applied it to nonlifting symmetric supercritical flow past a biconvex profile. A related application was reported in Ref. 1 for a symmetric nonlifting cascade. Extensions were later made to two-dimensional lifting flows[3,4] and preliminary applications made to three-dimensional[3,5] flows. The concept was applied to perturbation of both physical parameters,[1-5] namely, geometry or flow variables, and nonphysical parameters,[5] such as grid size or level of governing equation. In total, these initial applications served to establish the overall applicability of the approximation concept. In view of the potential of the method for providing substantial computational savings for a wide spectrum of nonlinear problems, the work reported here focuses on a detailed evaluation of the method. Results are presented that illustrate the accuracy and limits of validity that can be expected in typical applications, and provide some guidelines on how best to apply the method.

A crucial aspect of such a method is its ability to treat accurately regions where either discontinuities or high gradients exist. The concept of coordinate straining suggested by Nixon[2,3] to account for the displacement of discontinuities due to parameter changes is used here and is extended to predict displacements of other high gradient locations such as stagnation points, maximum suction pressure points, etc. The question of nonuniqueness of the straining function and its effect on the approximation predictions is examined. An example of employing two different straining functions for a strongly supercritical flow was provided in Ref. 3 and displayed no difference in results. Here we provide additional results which do exhibit differences and demonstrate the limitations of certain classes of straining functions.

Although the methodology developed is applicable to general nonlinear problems, the specific results reported are for aerodynamic applications. Single and simultaneous multiple parameter perturbation results based on transonic small disturbance and full potential solutions are presented for nonlinear transonic flows past both isolated airfoils and compressor cascades. In order to enable a critical evaluation of the procedure, emphasis is placed on strongly supercritical flows which exhibit large surface shock movement over the parametric range studied.

Analysis

Approximation Concept

The basic hypothesis underlying the present procedure is that a range of solutions in the vicinity of a previously determined or base solution can be calculated to first-order accuracy in the incremental change of the varied parameter by determining a linearized unit perturbation solution Q_p defined according to the relation

$$Q = Q_0 + \Delta\{Q_p\} \tag{1}$$

where Q is the approximate solution for conditions differing from the base solution Q_0 by an amount Δ of some arbitrary

Received Oct. 26, 1980; revision received Dec. 17, 1981.

*Department Manager, Theoretical Fluid Mechanics. Associate Fellow AIAA.

†Research Scientist; currently with Compression Labs, Inc., San Jose, Calif.

‡Professor, Division of Applied Mechanics; consultant Nielsen Engineering and Research, Inc. Fellow AIAA.

flow quantity. The effectiveness of such an approximation method depends upon the ability of the relationship in Eq. (1) to remain accurate over a range Δ of practical significance, and the fact that Q_p need be determined only once.

For the approximation method, Q_p is determined simply by differencing two nonlinear base flow solutions removed from one another by some nominal change of a particular flow or geometrical quantity and then dividing that result by the change in the perturbed quantity. Related solutions are obtained by multiplying the unit perturbation by the desired parameter change and adding that result to the base flow solution. This simple procedure, however, only works directly for continuous flows for which the perturbation change does not alter the solution domain. For those perturbations that change the flow domain, coordinate stretching (usually obvious) is necessary to insure proper definition of the unit perturbation solution. For discontinuous flows, coordinate straining is necessary to account additionally for movement of discontinuity due to the parameter change.

The attractiveness of the approximation method is that it is not restricted to a linear variation range but rather replaces the nonlinear variation between two base solutions with a linear fit. This de-emphasizes the sensitivity inherent in the classical linear perturbation equation approach. Moreover, other than the approximation of a linear fit between two nonlinear base solutions, the method is not restricted by further approximations with respect to the governing differential equations and boundary conditions. Rather, it retains the full character of the original methods used to calculate the base flow solutions. Most importantly, no perturbation differential equations have to be posed and solved, only algebraic ones. In fact, it is not necessary to know the exact form of the perturbation equation, only that it can be obtained by some systematic procedure and the perturbations thus defined will behave in some "generally appropriate" fashion so as to permit a logical perturbation analysis. For situations involving perturbations of physical parameters, such as reported here, the governing perturbation equations are usually transparent, or at least readily derivable. Finally, because of the implicit nature of coordinate straining, the approximation solution is nonlinear in the varied parameter.

The primary disadvantage of the method is that two base solutions are required for each parameter perturbation considered. Furthermore, both flows must be topologically similar, i.e., discontinuities or other characteristic features must be present in both base solutions used to establish the unit perturbation.

Coordinate Straining

The concept of employing coordinate straining to remove nonuniformities from perturbation solutions of nonlinear problems is well established and was originally suggested by Lighthill[6] three decades ago. The basic idea of the technique is that a straightforward perturbation solution may possess the appropriate form, but not quite at the appropriate location. The procedure is to strain slightly the coordinates by expanding them as well as the dependent variables in an asymptotic series. It is often unnecessary to actually solve for the straining. It generally can be established by inspection. The final uniformly valid solution is then found in implicit form, with the strained coordinate appearing as a parameter.

In the original applications of the method,[7] it was applied in the "classical" sense; that is, series expansions of the dependent and independent variables in ascending powers in some small parameter were inserted into the full governing equation and boundary conditions, and the individual terms of the series determined. An ingenious variation in the application of the method was made by Pritulo[8] who demonstrated that if a perturbation solution in unstrained coordinates has been determined and found to be nonuniform, the coordinate straining required to render that solution uniformly valid can be found by employing straining directly in the known nonuniform solution, and then solving algebraic rather than differential equations. The idea of introducing strained coordinates a posteriori has since been applied to a variety of different problems[7] and forms the basis of the current application.

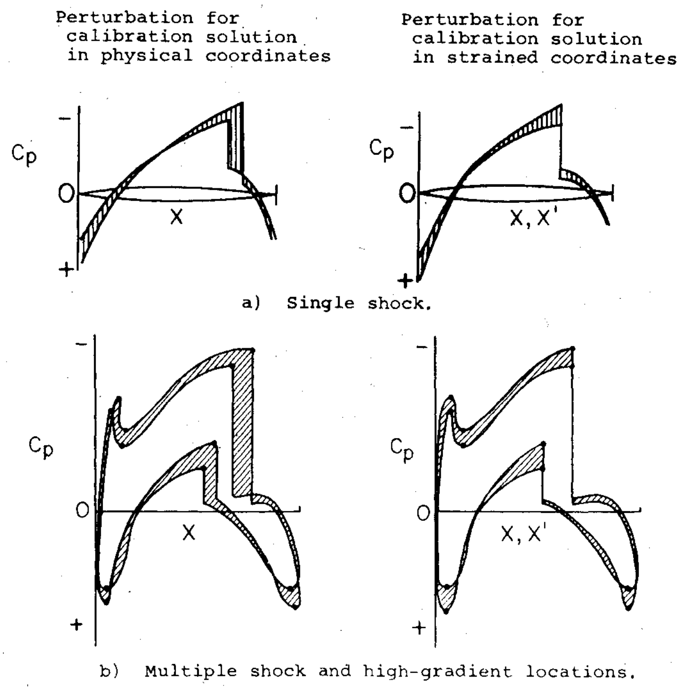

Fig. 1 Perturbation solution for calibration solution in physical and strained coordinates.

The fundamental idea underlying coordinate straining, as it relates to the present aerodynamic applications, is illustrated graphically in Fig. 1. In the upper plot on the left, two typical transonic pressure distributions are shown for a highly supercritical flow about a nonlifting symmetric profile. The distributions can be regarded as related nonlinear flow solutions separated by a nominal change in some geometric or flow parameter. The shaded area between the solutions represents the perturbation result that would be obtained by directly differencing the two solutions. We observe that the perturbation so obtained is small everywhere except in the region between the two shock waves, where it is fully as large as the base solutions themselves. This clearly invalidates the approximation technique in that region and most probably somewhat ahead and behind it as well. The key idea for correcting this, pointed out by Nixon,[2,3] is first to strain the coordinates of one of the two solutions in such a fashion that the shock waves align, as shown in the upper plot on the right of Fig. 1, and then determine the unit perturbation. Equivalently, this can be considered as maintaining the shock-wave location invariant during the perturbation process, and assures that the unit perturbation remains small both at and in the vicinity of the shock wave. Obviously, shock points are only one of a number of characteristic high gradient locations such as stagnation points, maximum suction pressure points, etc., in which the accuracy of the approximation solution can degrade rapidly. The plots in the lower left part of the Fig. 1 indicate such a situation which contains multiple shocks and high gradient regions. Simultaneously straining all these locations, as indicated in the lower right plot, serves to *minimize* the unit perturbation over the entire domain considered and provides the basis of the high accuracy of the method.

Because the method of strained coordinates is known to be nonapplicable to certain classes of perturbation problems, or worse, appear to be applicable while producing incorrect results,[7] the point arises as to its use in the present context.

The question is not whether the method will produce a uniformly valid solution—the expansion procedure guarantees that—but whether the solution so produced may be incorrect inherently. Unfortunately, unlike the method of matched asymptotic expansions, there are no firm rules which guarantee the correctness of strained coordinate solutions. There are, nevertheless, some generally reliable guidelines. The method of strained coordinates appears to always succeed when the singularity predicted by the direct unstrained problem actually exists. In our applications, this is always the case, since we identify the singularity or invariant points as shock points, stagnation points, and other physically identifiable points. Furthermore, we restrict the allowable range of parametric variation such that the neighboring calibration and predicted flows retain these same points and create no new ones. Therefore, invariant points are neither lost nor generated over the solution domain of interest. These considerations effectively insure that the predicted approximation solutions will both be physically correct and, additionally, will not violate the basic straining principle[7] regarding compounding of singularities.

Analytical Formulation

In order to provide the theoretical essentials of the method, consider the formulation of the procedure at the level of the full potential equation. We denote the operator L acting on the velocity potential equation for Φ as that which results in the two-dimensional full potential equation for Φ, i.e.,

$$L[\Phi]=0 \tag{2}$$

If we now expand the potential in terms of zero and higher-order components in order to account for the variation of some arbitrary geometrical or flow parameter q

$$\Phi=\Phi_0+\epsilon\phi_1+\ldots; \qquad q=q_0+\Delta q \tag{3}$$

and then insert this into the governing Eq. (2), expand the result, order the equations into zero- and first-order components, and make the obvious choice of expansion parameter $\epsilon=\Delta q$, we obtain the following governing equations for the zero- and first-order components:

$$L[\Phi_0]=0; \qquad L_1[\Phi_1]+\frac{\partial}{\partial q}L[\Phi_0]=0 \tag{4}$$

Here L_1 is a linear operator whose coefficients depend on zero-order quantities and $\partial L[\Phi_0]/\partial q$ represents a "forcing" term due to the perturbation. Actual forms of L_1 and the forcing term are provided in Ref. 1 for a variety of flow and geometry parameter perturbations of a two-dimensional turbomachine, and in Ref. 4 for profile shape perturbations of an isolated airfoil. An important point regarding Eq. (4) for the first-order perturbation Φ_1 is that the equation represents a unit perturbation independent of the actual value of the perturbation quantity ϵ.

Appropriate account of the movement of discontinuities and maxima of high gradient regions due to the perturbation now is accomplished by the introduction of strained coordinates (s,t) in the form

$$x=s+\epsilon x_1(x,t); \qquad y=t+\epsilon y_1(s,t) \tag{5}$$

where

$$x_1(x,t)=\sum_{i=1}^{N}\delta x_i x_{1_i}(s,t); \quad y_1(x,t)=\sum_{i=1}^{N}\delta y_i y_{1_i}(s,t) \tag{6}$$

and $\epsilon\delta x_i$, $\epsilon\delta y_i$ represent individual displacements of the N strained or invariant points, and $x_{1_i}(s,t)$, $y_{1_i}(s,t)$ are straining functions associated with each of the N invariant points. Introducing the strained coordinates Eqs. (5) and (6) into the expansion formulation leaves the zero-order result in Eq. (4) unchanged, but results in a change of the following form for the first-order term:

$$L_1[\Phi_1]+L_2[\Phi_0]+\frac{\partial}{\partial q}L[\Phi_0]=0 \tag{7}$$

Here the operators are understood to be expressed in terms of the strained (s,t) coordinates, and the additional operator L_2 arises specifically from displacement of the strained points. In Refs. 3 and 4 specific expressions for L_2 are provided for selected perturbations involving transonic small disturbance and full potential formulations. The primary point, however, with regard to Eq. (7) expressed in strained coordinates is that it remains valid as before for a unit perturbation and independent of ϵ.

In employing the approximation method, Eq. (7) for the unit perturbation is solved by taking the difference between two solutions obtained by the full nonlinear procedure after appropriately straining the coordinates. If we designate the two solutions for some arbitrary flow quantity q as base Q_0 and calibration Q_c, respectively, of the varied parameter, we have for the predicted flow at some new parameter value q (Ref. 5)

$$Q(x,y)=Q_0(s,t)=(\epsilon/\epsilon_0)[Q_c(\bar{x},\bar{y})-Q_0(s,t)] \tag{8}$$

where

$$\bar{x}=s+\epsilon_0 x_1(s,t); \qquad \bar{y}=t+\epsilon_0 y_1(s,t)$$
$$x=s+(\epsilon/\epsilon_0)[\bar{x}-s]; \qquad y=t+(\epsilon/\epsilon_0)[\bar{y}-t]$$
$$\epsilon_0=q_c-q_0; \qquad \epsilon=q-q_0 \tag{9}$$

Extension of this result to simultaneous multiple parameter perturbations is straightforward[3]; and that extension is provided in the following section where applications of the approximation procedure are made to predict surface properties. Also provided are the particular forms of the straining functions Eq. (5) for those applications.

Application to Surface Properties

For the current applications, we have employed coordinate straining with the approximation method to predict surface pressure distributions for a wide variety of single and multiple parameter geometrical and flow perturbations of isolated airfoils and cascades. In that instance where flow properties are required along some contour, the first-order solutions can be represented by

$$Q(x;\epsilon_j)=Q_0(s)+\sum_{j=1}^{M}\epsilon_j Q_{1_j}(s)$$
$$x=s+\sum_{j=1}^{M}\epsilon_j x_1(s) \tag{10}$$

where x is the independent variable measuring distance along the contour or a convenient projection of that distance, s is the strained coordinate, and ϵ_j a small parameter representing the change in one of M flow or geometrical variables which we wish to vary simultaneously.

In order to determine the first-order corrections $Q_{1_j}(s)$, we require one base and M calibration solutions in which the calibration solutions are determined by individually varying each of the M parameters by some nominal amount from the base flow value while keeping the others fixed at their base flow values.

In this way, the first-order corrections $Q_{1_j}(s)$ can be represented as

$$Q_{1_j}(s) = [Q_{c_j}(\bar{x}_j) - Q_0(s)]/\epsilon_j^c \tag{11}$$

where Q_{c_j} is the calibration solution corresponding to changing the jth parameter q_j to a new value q_{c_j}, $\bar{x}_j$ is the strained coordinate pertaining to the Q_{c_j} calibration solution, and ϵ_j^c represents the change $q_{c_j} - q_{0_j}$ in the jth parameter from its base flow value. If we now desire to keep invariant during the perturbation process a total of N points corresponding to discontinuities or high gradient maxima, the coordinates $\bar{x}_j$ and x can be given by

$$\bar{x}_j = s + \sum_{i=1}^{N} \epsilon_j^c (\delta x_i^c)_j x_{1_i}(s) \tag{12}$$

$$x = s + \sum_{j=1}^{M}\sum_{i=1}^{N} \epsilon_j (\delta x_i^c)_j x_{1_i}(s) \tag{13}$$

where

$$\epsilon_j^c = q_{c_j} - q_{0_j}; \qquad \epsilon_j = q_j - q_{0_j} \tag{14}$$

$$\epsilon_j^c(\delta x_i^c)_j = (x_i^c - x_i^0)_j; \quad \epsilon_j(\delta x_i^c)_j = (\epsilon_j/\epsilon_j^c)(x_i^c - x_i^0)_j \tag{15}$$

Here $\epsilon_j^c(\delta x_i^c)_j$ given in Eqs. (12) and (15) represents the displacement of the ith invariant point in the jth calibration solution from its base flow location due to the selected change ϵ_j^c in the q_j parameter given in Eq. (14); $\epsilon_j(\delta x_i^c)_j$ given in Eqs. (13) and (15) represents the predicted displacement of the ith invariant point from its base flow location due to the desired change ϵ_j in the q_j parameter given in Eq. (14); and $x_{1_i}(s)$ is a unit order straining function having the property that

$$x_{1_i}(x_k^0) = \begin{cases} 1 & k = i \\ 0 & k \neq i \end{cases} \tag{16}$$

which assures alignment of the ith invariant point between the base and the calibration solutions.

In addition to the single condition Eq. (16) on the straining function, it may be convenient or necessary to impose additional conditions at other locations along the contour. For example, it is usually necessary to hold invariant the end points along the contour, as well as to require that the straining vanish in a particular fashion in those locations. All of these conditions, however, do not serve to determine the straining uniquely. The nonuniqueness of the straining, nevertheless, often can be turned to advantage, either by selecting particularly simple classes of straining functions, or by requiring the straining to satisfy further constraints convenient for a particular application.

In the present application, the problem posed for the first-order strained coordinate approximation is somewhat unusual in that the straining requirements are fixed a priori rather than determined as part of the solution. Consequently, it is unnecessary to examine a higher-order straining problem as is the standard procedure[7] for determining the straining. Rather, the straining is established on the basis of Eq. (16) regarding displacement of the invariant points. Since relatively simple classes of straining functions can accomplish this, the results obtained thus far with the approximation method have employed either various continuous polynomial straining functions or piecewise continuous linear straining functions.

The fact of nonuniqueness of straining functions, however, raises a further question of the dependence of the final approximation predicted result on choice of straining function.

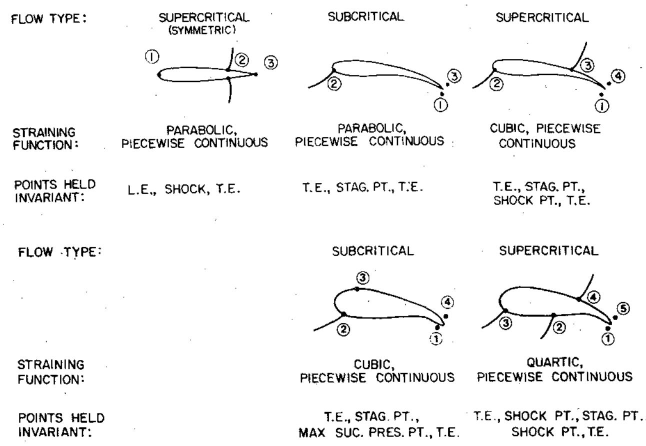

Fig. 2 Summary of various flows and straining functions considered.

An initial example of the effect of employing two different straining functions for a strongly supercritical flow was provided in Ref. 3. Those results indicated no difference between the two approximation solutions. In Ref. 9, it was demonstrated that the final approximation result when employing strained coordinates in the present manner is formally independent of the particular straining function used, provided the function moves the invariant points to the proper locations. We have found this to be true for predictions at and in the vicinity of invariant points. However, we have also found that certain classes of straining functions can have the undesirable property of causing unwanted straining in regions removed from the invariant points. This has the effect of inducing spurious behavior in the approximation predictions in those regions. Here we provide examples of such results, and demonstrate in particular some of the limitations of various polynomial straining functions in comparison with piecewise continuous functions.

For continuous polynomial and linear piecewise continuous straining, the functional forms of the straining can be written compactly. For example, Eq. (12) becomes, for continuous polynomial straining

$$\bar{x}_j = s + \sum_{i=2}^{N-1} L_i(s)(x_i^c - x_i^0)_j \tag{17}$$

where L_i are Lagrangian coefficients given by

$$L_i(s) = \prod_{\substack{k=1\\k\neq i}}^{N} \frac{(s - x_k^0)}{(x_i^0 - x_k^0)} \tag{18}$$

whereas for linear piecewise continuous straining, $\bar{x}_j$ is given by

$$\bar{x}_j = x + \left\{ \frac{x_{i+1}^0 - s}{x_{i+1}^0 - x_i^0}(x_i^c - x_i^0)_j + \frac{s - x_i^0}{x_{i+1}^0 - x_i^0}(x_{i+1}^c - x_{i+1}^0)_j \right\} H(x_{i+1}^0 - s) H(s - x_i^0) \tag{19}$$

where H denotes the Heaviside step function. As discussed earlier, it is usually necessary to hold invariant both of the end points along the contour in addition to the points corresponding to discontinuities or high gradient maxima. For the results reported here, the array of invariant points in the base and calibration solutions have been chosen as

$$x_i^0 = \{0, x_1^0, x_2^0, \ldots, x_n^0, 1\} \qquad x_{i_j}^c = \{0, x_1^c, x_2^c, \ldots, x_n^c, 1\}_j \tag{20}$$

where the contour length has been normalized to one. Figure 2

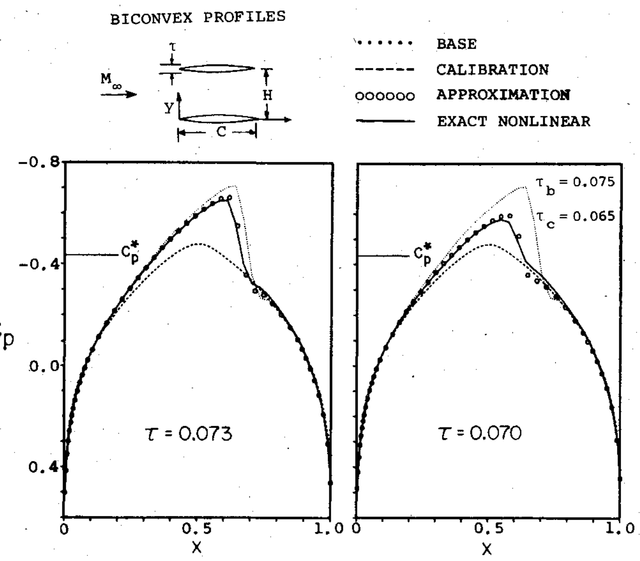

Fig. 3 Comparison of approximation and nonlinear surface pressures for a thickness ratio perturbation of a nonlifting cascade of biconvex profiles with $H/C = 1.0$ at $M_\infty = 0.80$.

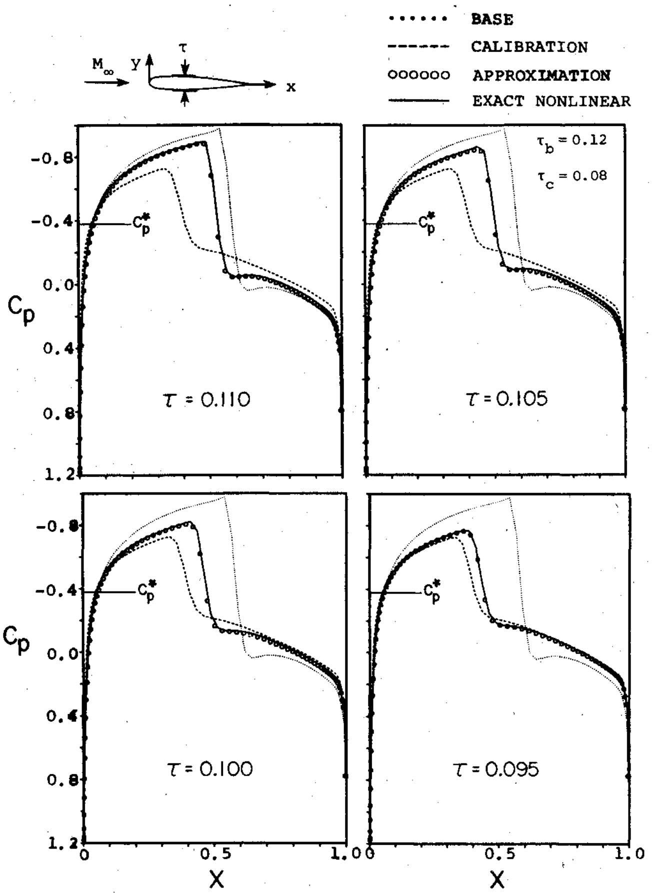

Fig. 4 Comparison of approximation and nonlinear surface pressures for a thickness ratio perturbation for an isolated NACA four-digit airfoil at $M_\infty = 0.820$ and $\alpha = 0$ deg for solution interpolation.

provides a summary of the combinations of flows and straining functions studied.

Results

One of the primary objectives of the present investigation is to explore the accuracy and range of validity of such approximation procedures to determine to what extent they are capable of providing results useful in an engineering analysis. To this end, we have tested the method in a variety of different geometrical and flow condition perturbations, including applications of both isolated airfoils and compressor cascades. Since the ability of the method to account accurately for the movement of discontinuities and maxima of high gradient regions is essential if such procedures are to be of general use, emphasis was placed on transonic flows that are strongly supercritical and exhibit large surface shock movement over the parametric range studied. Base flow theoretical solutions were determined from small-disturbance transonic potential[10] and full potential solutions.[11,12] In the results to follow, which were selected as typical from systematic calculations of a much larger number of cases, the choice of base and calibration solutions was often made at the limits of validity of the procedure to observe how well the method performs under such conditions.

Single Parameter Perturbations

In Fig. 3, we present results for a thickness ratio perturbation of strongly supercritical flows past a nonlifting cascade of biconvex profiles at $M_\infty = 0.8$ having a spacing to chord ratio of $H/C = 1.0$. The dotted and dashed results on the figure represent the base and calibration surface pressure distributions for $\tau = (0.075, 0.065)$, respectively, and were obtained by solving the transonic small-disturbance potential equation using the code TSFOIL.[10] An x grid having 48 points on the blade profile was used. These solutions, then, were used to determine the unit perturbation. The open circles represent the approximation solution for $\tau = 0.073$ in the plot on the left and for $\tau = 0.070$ in the plot on the right. Those results are meant to be compared with the solid lines in the plots that are the corresponding nonlinear solutions obtained by rerunning TSFOIL at the new thickness ratios. Quadratic straining was used with shock point and leading and trailing edges held invariant. The base and calibration flow shock-point locations for this example, as well as for all of the supercritical cases presented here, were determined as the point where the pressure coefficient passed through critical with compressive gradient.

With regard to the results, several points are noteworthy. Selection of a cascade rather than an isolated airfoil provides a more sensitive transonic flow situation. Additionally, the choice of a highly supercritical base and almost subcritical calibration solution provides both an example of extreme separation between the two nonlinear solutions used to define the unit perturbation, as well as a situation where one solution is near the limits of validity of the perturbation analysis. Recall that both solutions must be topographically similar, i.e., must contain the same number of discontinuities (shocks) and other characteristic features.

We note that comparisons of the approximation results with the nonlinear calculations are very satisfactory for both thickness ratios, with the only discrepancy being a slight disagreement at the lower thickness ratio ($\tau = 0.070$) at several points in the postshock region. Additional calculations, not presented here, in which a more reasonable choice of calibration solution is made, say at $\tau = 0.070$, removes that discrepancy. The main point provided by the results of Fig. 3 is that for certain classes of supercritical flows even widely separated base solutions can be used to provide accurate approximation predictions.

In Fig. 4, we provide similar strongly supercritical results again for interpolation-only approximation solutions, but on a somewhat finer grid. These results employed full potential base solutions,[11] and represent thickness ratio perturbations of nonlifting symmetric free air flows past NACA four-digit thickness only airfoils at $M_\infty = 0.820$. The body-fitted mesh employed had 75 points on both upper and lower surfaces, which is half again as many as in the preceding example. For the base and calibration flows, the thickness ratios were $\tau = 0.120$ and 0.080, respectively. Comparisons between the

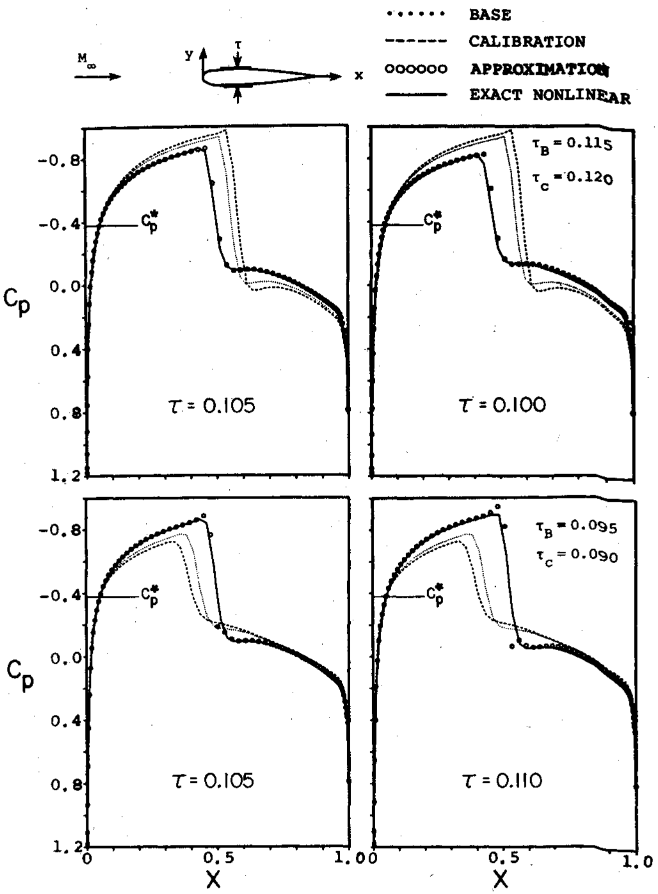

Fig. 5 Comparison of approximation and nonlinear surface pressures for a thickness ratio perturbation for an isolated NACA four-digit airfoil at $M_\infty = 0.820$ and $\alpha = 0$ deg for extreme solution extrapolation.

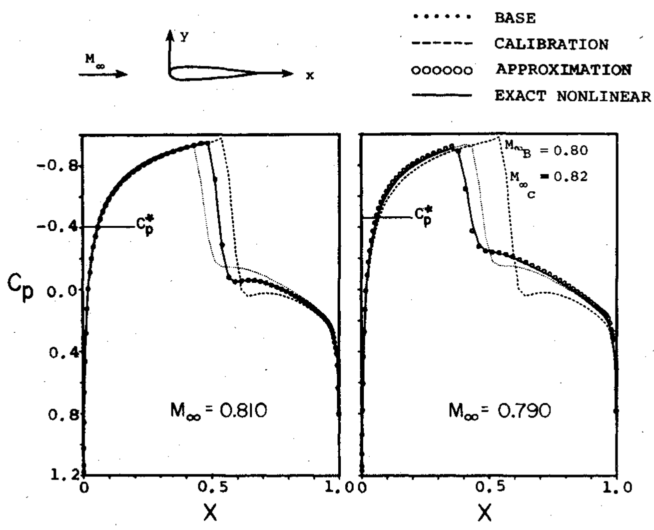

Fig. 6 Comparison of approximation and nonlinear surface pressures for a Mach number perturbation of an isolated NACA 0012 airfoil at $\alpha = 0$ deg.

approximation predictions and the full nonlinear calculations are exhibited in Fig. 4 for $\tau = 0.110$, 0.105, 0.100, and 0.095. We note that the comparisons are remarkably good, in particular, in the region of the shock. The first-order approximation results accurately predict both shock location and post-shock expansion behavior. Reference to the coarser grid results given in Fig. 3 indicates that the finer grid resolution clearly enhances the predictions, indicating that better accuracy and a larger range of validity can be anticipated when fine grid solutions are used to define the unit perturbation.

In the two preceding examples, approximation results were provided for interpolation between widely spaced base and calibration solutions. In Fig. 5, we provide similar strongly supercritical thickness ratio perturbation results for extreme extrapolation using very closely spaced base and calibration solutions.[11] The upper plots display results for extrapolation downward from base and calibration flows past nonlifting NACA four-digit profiles with $\tau = 0.115$ and 0.120 at $M_\infty = 0.820$. Approximation predictions are shown for $\tau = 0.105$ and 0.100, which represent $\Delta\tau$ excursions from the base flow ($\tau = 0.115$) that are two and three times the parameter change between the base and calibration solutions ($\Delta\tau = 0.005$) used to define the unit perturbation. For these results, comparisons with full nonlinear calculations are very good. The lower plots display similar results for extreme extrapolation upward from base and calibration solutions having $\tau = 0.095$ and 0.090. Approximation predictions are shown for $\tau = 0.105$ and 0.110, which again represent excursions from the base flow that are two and three times the parameter change between the base and calibration solutions. In this instance, while comparisons of the approximation results and the full nonlinear solutions for both cases are good, the results at $\tau = 0.110$ are beginning to display some not surprising discrepancies near the shock wave, indicating that the approximation result is nearing the limit of its range of validity for this particular choice of base and calibration flows.

The results indicated in Fig. 5, however, clearly demonstrate that not only is accurate solution extrapolation possible, but that for some situations even closely spaced nonlinear solutions can be used to cover a wide range of related solutions. Additionally, the range of parameter variation in this example over which the approximation results remain accurate—i.e., parameter changes three times the difference between the two nonlinear solutions used to define the unit perturbation—is remarkable, and far beyond what one would anticipate for a first-order correction.

Approximation results using a more reasonable choice of base and calibration solutions and using a flow rather than geometry parameter are provided in Fig. 6. Those results involve Mach number perturbations of highly supercritical full potential[11] flows past a NACA 0012 airfoil at $\alpha = 0$ deg. The base and calibration results are for $M_\infty = 0.800$ and 0.820, and the comparisons indicated are for interpolation to $M_\infty = 0.810$ and extrapolation downward to $M_\infty = 0.790$. As with the previous geometric perturbations, these results are similarly in very good agreement with the nonlinear calculations. For these cases, as well as for a number of other Mach number perturbations, we have separately determined the approximation prediction in two different ways. First, we have taken cognizance of the fact that a Mach number perturbation alters the governing differential equation for the first-order perturbation from that of other geometric or flow parameter changes; and have used the suggestion of Ref. 3 to consider such perturbations via a transonic small-disturbance approximation, whereby the same perturbation equation can be preserved by employing a modified expansion parameter ϵ. An alternative procedure is to treat a Mach perturbation directly and interpret ϵ as the difference in Mach number. We have done both of these calculations and compared the perturbation results for a number of cases using both full potential solutions, as for the results shown in Fig. 6, and transonic small-disturbance solutions, and have observed no essential difference between the two sets of results. The approximation results presented in Fig. 6 correspond to those for ϵ equal to the difference in Mach number.

In Fig. 7, we present results for an angle-of-attack perturbation of lifting flows past a NACA 0012 profile at $M_\infty = 0.70$. The full potential[11] base and calibration solutions

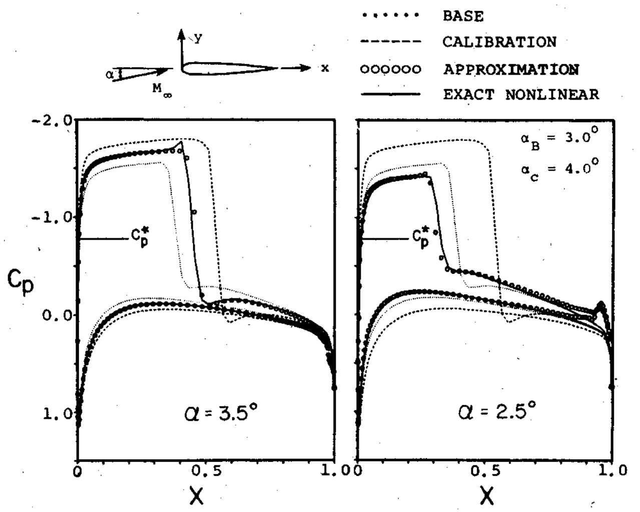

Fig. 7 Comparison of approximation and nonlinear surface pressures for an angle-of-attack perturbation of an isolated NACA 0012 airfoil at $M_\infty = 0.70$.

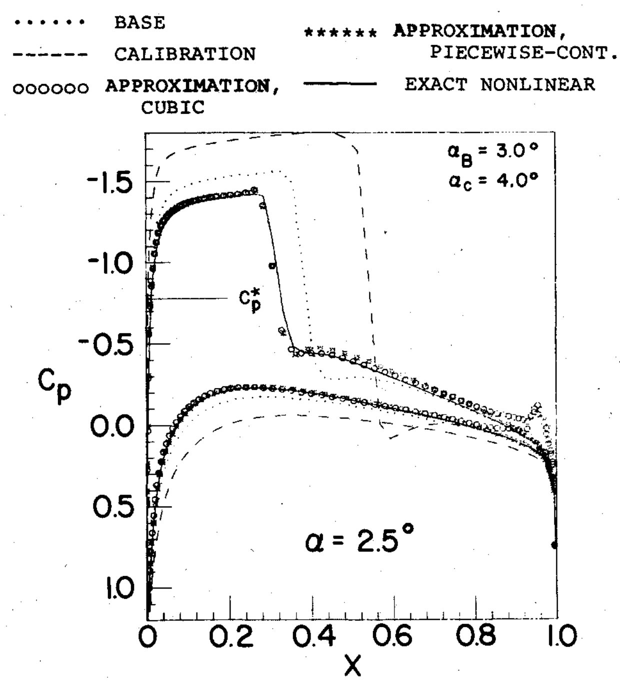

Fig. 8 Comparison of nonlinear surface pressures with approximation results using cubic or linear piecewise continuous straining functions for an angle-of-attack perturbation of an isolated NACA 0012 airfoil at $M_\infty = 0.70$.

are at $\alpha = 3.0$ and 4.0 deg with comparisons of approximation and nonlinear results at $\alpha = 3.5$ and 2.5 deg. Cubic straining has been used with the invariant points corresponding to the lower trailing edge, stagnation point, shock point, and the upper trailing edge (see Fig. 2). We note that for $\alpha = 3.5$ deg, the approximation results are very good everywhere, in particular, in the vicinity of the shock and stagnation regions. At $\alpha = 2.5$ deg, the approximation results are still very good in the shock and stagnation regions and on most of the upper and lower surface, but near the trailing edge a discrepancy has occurred. The cause lies solely with the straining function (cubic) used. Although the straining vanishes identically at the trailing edge, for the particular choice of base and calibration solutions in this example, the straining in the near vicinity of the trailing edge is sufficiently large to introduce a misalignment in the unit perturbation. The correction to this is discussed in the following section.

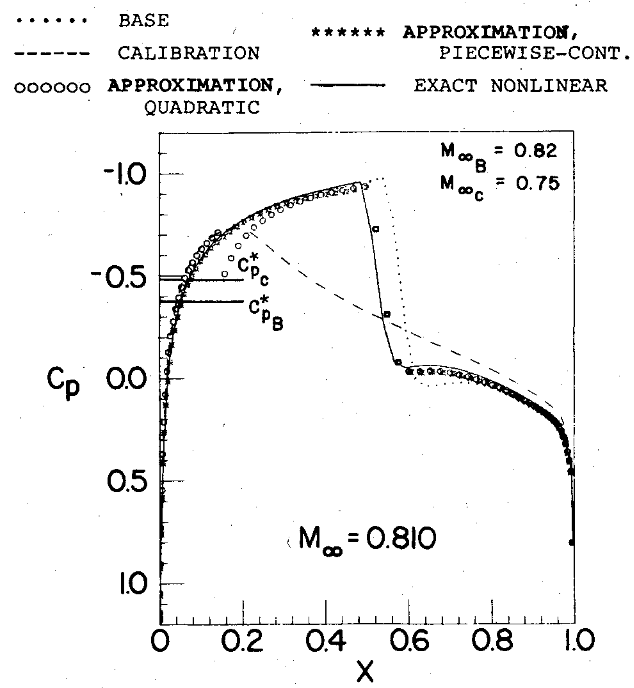

Fig. 9 Comparison of nonlinear surface pressures with approximation results using quadratic or linear piecewise continuous straining functions for a Mach number perturbation of an isolated NACA 0012 airfoil at $\alpha = 0$ deg.

Piecewise Continuous Straining Functions

The results presented in Figs. 8 and 9 illustrate the effect of using different classes of straining functions to determine the approximation results, and highlight, in particular, certain limitations with continuous polynomial straining functions. Comparisons are provided for two strongly supercritical flows, and demonstrate the differences between continuous quadratic and cubic straining functions and corresponding piecewise continuous straining functions.

Figure 8 displays a comparison for a supercritical angle-of-attack perturbation at $\alpha = 2.5$ deg for which results based on cubic straining were given in Fig. 7. The open circles denote the previously obtained cubic straining approximation result, while the asterisks denote the corresponding result when using linear piecewise continuous straining. For both straining functions, the invariant points are the lower trailing edge, stagnation point, shock point, and the upper trailing edge. We note that the spurious behavior near both the upper and lower surface trailing edge caused by unwanted straining in the cubic result has been corrected by piecewise continuous straining. Most importantly, the piecewise continuous result indicates very good agreement with the full nonlinear solution in that region. Furthermore, the good agreement with the full nonlinear result which the cubic result displayed near the shock and stagnation regions is also obtained with the piecewise continuous result. In fact, with the exception of the trailing edge region, both straining results are essentially identical. This example illustrates the typical independence of the approximation prediction on straining function at and in the vicinity of invariant points, as well as in regions where no excessive straining is introduced by a particular straining function.

In addition to excess straining at locations removed from invariant points, we have found that continuous polynomial straining can, in certain cases, actually strain points off the contour surface, particularly when large shock displacements are involved. This, of course, invalidates the determination of the unit perturbation, and requires that a different straining function be employed. Piecewise continuous linear straining functions again provide a simple means of avoiding such difficulties.

In Fig. 9, we provide an example illustrating this effect for a quadratic straining function. There a comparison is made of approximation results obtained using quadratic (open circles) and linear piecewise continuous (asterisks) straining applied to a supercritical Mach number perturbation for symmetric nonlifting flow past a NACA 0012 airfoil. Widely separated base/calibration flows[11] at $M=0.820$ and 0.750 were used to predict the flow at $M_\infty=0.810$. The invariant points are the leading edge, shock point, and trailing edge. The spurious behavior near $x=0.16$ displayed by the open circles is due to the quadratic function moving points in the strained calibration solution of the airfoil surface. The piecewise continuous results indicated by the asterisks display a smooth variation in that region, and provide good agreement everywhere with the full nonlinear result. Note again the close agreement at and near the shock between the two approximation predictions, indicating independence of straining function at that invariant point.

Further comparisons of continuous polynomial and piecewise continuous approximation predictions have been made and are reported in Ref. 13. The essential conclusions from all of these results are that the approximation predictions are independent of straining function when invariant point displacement between base, calibration, and predicted solution is modest. For the more important cases involving larger displacements, continuous polynomial straining can introduce spurious results. Linear piecewise continuous straining provides a simple and direct means of avoiding this, and has proven effective and accurate in all case studies undertaken.

Multiple Parameter Perturbations

All of the previous results presented are for single parameter perturbations of some flow or geometry parameter. In Figs. 10 and 11, we provide corresponding results for the simultaneous perturbation of two or more parameters. In Fig. 10, comparisons are provided for the simultaneous perturbation of thickness ratio and oncoming Mach number of highly supercritical full potential[11] flows past NACA four-digit airfoils. The base flow was chosen at $M_\infty=0.820$ and $\tau=0.120$ and is displayed as the dotted line in both plots. The calibration flow selected to account for M_∞ changes is at $M_\infty=0.800$ and $\tau=0.120$ and is displayed in the plot on the left; while the calibration flow for thickness ratio changes is at $M_\infty=0.820$ and $\tau=0.110$ and is displayed in the plot on the right. The comparison between the approximation and exact nonlinear results are for parameter extrapolation to $M_\infty=0.790$ and $\tau=0.115$. Note that the indicated results for base, approximation, and exact nonlinear solution in both plots of Fig. 10 are the same; the primary reason for presenting two plots is to indicate clearly the separation between the base, the two calibration solutions, and the predicted result. The straining employed is linear piecewise continuous, with leading and trailing edge and shock point held invariant. With regard to the results, the comparison between the approximation and the exact nonlinear results is extremely good, in particular in the region of the shock. We note that the parameter values of (M_∞,τ) selected for the prediction solution represent relatively substantial excursions from the base and calibration values. Nevertheless, the approximation method is able to predict the solution accurately.

The final result provided in Fig. 11 is for a four parameter perturbation of strongly supercritical full potential[12] flows past a cascade of compressor blades having NACA four-digit profiles. The base flow is for an oncoming Mach number of $M_\infty=0.78$, thickness ratio $\tau=0.110$, gap-to-chord ratio $t=3.2$, and oncoming inflow angle $\alpha=0.3$ deg. The four calibration solutions to account for changes in these parameters involved individually varying each parameter from its base value to its calibration matrix value given by $\{M_\infty, \tau, t, \alpha\}=\{0.790, 0.120, 3.0, 0.5 \text{ deg}\}$ while keeping the others at their base values. Comparison of predicted and exact

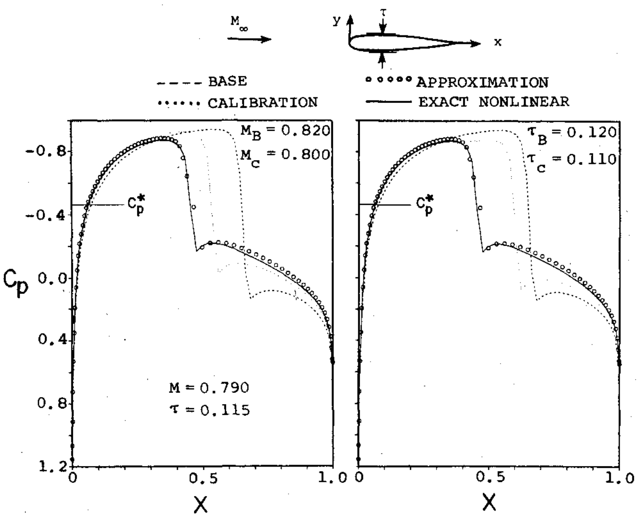

Fig. 10 Comparison of approximation and nonlinear surface pressure for simultaneous Mach number and thickness ratio perturbation of a nonlifting isolated NACA four-digit airfoil.

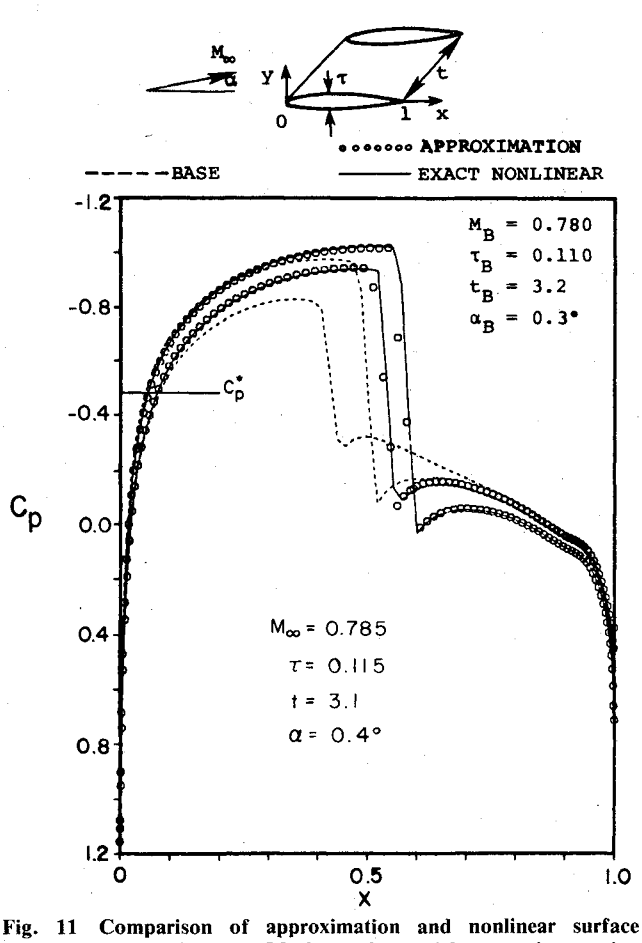

Fig. 11 Comparison of approximation and nonlinear surface pressures for simultaneous Mach number, thickness ratio, spacing ratio, and oncoming flow angle perturbation of a cascade of NACA four-digit blades.

nonlinear results are for parameter values of $\{M_\infty, \tau, t, \alpha\}=\{0.785, 0.115, 3.1, 0.4 \text{ deg}\}$. The base solution is indicated as the dashed line and provides some idea of the solution displacement. The four calibration solutions are not shown. This particular set of flows was selected because of the presence of multiple shocks and high sensitivity to parameter change. Linear piecewise continuous straining was employed with the invariant points being the lower surface trailing edge, lower surface shock stagnation point, upper surface shock, and upper surface trailing edge. The comparisons between approximation and exact nonlinear results is again remarkably accurate. The predictions of both the locations of the shocks on the upper and lower surface are given very well, as are the pressure distributions in the regions immediately ahead and behind those shocks.

Concluding Remarks

An evaluation has been made of an approximation procedure for determining accurate approximations to families of nonlinear solutions that are either continuous or discontinuous, and that represent variations in some arbitrary parameter. The procedure employs two or more nonlinear solutions that differ from one another by a nominal change in some geometric or flow parameter to predict a family of related nonlinear solutions. Coordinate straining is used to account properly for the displacement of discontinuities and maxima of high-gradient regions. Extensive calculations, based on full potential nonlinear solutions and spanning a variety of flow and geometry perturbations of flows past isolated airfoils and compressor cascades, were carried out. Particular emphasis was placed on supercritical transonic flows which exhibit large surface shock movements over the parametric range studied. Approximation results, for both single and multiple parameter perturbations, characterized by both extreme solution interpolation and extrapolation, were obtained to exhibit the accuracy and range of validity of the method. Additionally, calculations investigating the effectiveness of linear piecewise continuous straining functions rather than continuous polynomial (quadratic, cubic, quartic) functions were carried out.

Comparisons of the approximation results with the corresponding exact nonlinear solutions indicate a remarkable accuracy of the method across the spectrum of examples reported. Use of fine grid base solutions clearly enhances approximation results particularly at discontinuities and high gradient regions. Solution interpolation and extrapolation are both feasible and accurate. Results evaluating the continuous polynomial and piecewise continuous straining functions indicate that the linear piecewise continuous functions are superior. Computational time of the method, beyond the determination of the base solutions, is trivial. Based on these results, we conclude that such a procedure can provide a means for substantially reducing computational requirements in design studies or other applications where large numbers of related nonlinear solutions are needed.

Acknowledgments

The results reported are based on research supported by NASA Lewis Research Center under Contract NAS3-20836 with Aaron Snyder as Technical Monitor.

References

[1] Stahara, S. S., Chaussee, D. S., and Spreiter, J. R., "Perturbation Solutions for Transonic Flow on the Blade-to-Blade Surface of Compressor Blade Rows," NASA CR-29-41, Jan. 1978.

[2] Nixon, D., "Perturbation of a Discontinuous Transonic Flow," *AIAA Journal,* Vol. 16, Jan. 1978, pp. 47-52.

[3] Nixon, D., "Perturbation in Two- and Three-Dimensional Transonic Flows," *AIAA Journal,* Vol. 16, July 1978, pp. 699-709.

[4] Nixon, D., "Design of Transonic Airfoil Sections Using a Similarity Theory," NASA TM 78521, Oct. 1978.

[5] Nixon, D., "Perturbation Methods in Transonic Flow," AIAA Paper 80-1367, July 1980.

[6] Lighthill, M. J., "A Technique for Rendering Approximate Solutions to Physical Problems Uniformly Valid," *Philosophical Magazine,* Vol. 40, 1949, pp. 1179-1201.

[7] Van Dyke, M., *Perturbation Methods in Fluid Mechanics,* The Parabolic Press, Calif., 1975.

[8] Pritulo, M. F., "On the Determination of Uniformly Accurate Solutions of Differential Equations by the Method of Perturbation Coordinates," *Journal of Applied Mathematics and Mechanics,* Vol. 26, 1962, pp. 661-667.

[9] Nixon, D. and McIntosh, S. C. Jr., "Further Observations on the Strained Coordinate Method for Transonic Flows," *AIAA Journal,* Vol. 18, Dec. 1980, pp. 1540-1541.

[10] Stahara, S. S., "Operational Manual for Two-Dimensional Transonic Code TSFOIL," NASA CR-3064, Dec. 1978.

[11] Holst, T. L. and Ballhaus, W. F., "Fast Conservative Schemes for the Full Potential Equation Applied to Transonic Flows," *AIAA Journal,* Vol. 17, Feb. 1979, pp. 145-152.

[12] Dulikravich, D. S., "CAS2D-FORTRAN Program for Nonrotating Blade-to-Blade, Steady, Potential Transonic Cascade Flows," NASA TP 1705, July 1980.

[13] Stahara, S. S., Elliott, J. P., and Spreiter, J. R., "A Rapid Perturbation Procedure for Determining Nonlinear Flow Solutions: Application to Transonic Turbomachinery Flows," NASA CR-3425, May 1981.